Lecture 10

Chemical State Imaging for Investigations of Neurodegenerative Disorders (Parkinsonism-Dementia Complex)

10.1. Introduction

Metallic elements, especially transition elements, appear to play an important role in neurodegenerative disorders such as Parkinson's disease (PD), Alzheimer's disease (AD), amyotrophic lateral sclerosis (ALS) and Guamanian parkinsonism-dementia complex (PDC) [1-5], based on findings of excessive accumulations of metallic elements in the brains of PDC cases, and iron in idiopathic Parkinson's disease [6-9] and Alzheimer's disease [10, 11]. The pathogenesis of the disease is still unknown, and researchers have suggested environmental factors as being of etiological importance [12, 13]. The "oxidative stress" hypothesis suggests that excessive transition metals can exchange electrons and change their valence which would promote production of free radicals that cause oxidative damage and neuronal degeneration [14-18]. Oxidative stress is defined as the strain of cellular function induced by reactive oxygen species (ROS), such as superoxide anions (O_2^-), hydroxyl radicals (OH^-), hydrogen peroxide (H_2O_2), and peroxynitrite ($ONOO^-$) [19]. ROS can induce lethal cellular damage through oxidation and peroxidation of proteins, lipids, and nucleic acids. Details of the relationships between transition metals and neuronal degeneration are still unclear. The distribution and chemical state of these metals is expected to give some insights into the understanding of pathogenic mechanism of these neurodegenerative disorders.

The distribution and metabolism of metallic elements such as iron have been investigated by using spectroscopic methods such as energy dispersive x-ray electron microprobe analysis [8,20], laser microprobe mass analyzer (LAMMA) [9], and nuclear micro probe [21]. These studies demonstrated the localization and distribution of iron in tissues from a patient with neurodegenerative disease, but these techniques cannot analyze the chemical state of the iron without homogenization or isolation.

Synchrotron radiation x-ray fluorescence (SR-XRF) spectrometry provides an alternative, powerful new tool for the investigation of trace elements [22]. It enables non-destructive analysis of the distributions, concentrations and chemical states at the cellular level of biological specimens with special high sensitivity and resolution [23-25]. Beside the fact that no fragmentation of the samples is required, the main advantage of this method lies in its non-invasive nature, as x-ray beams do not damage the samples. Therefore it is possible to conduct histological or histochemical analyses

by staining after the elemental analysis [26-28].

XANES spectroscopy provides the means to obtain information on the valence state and binding structure of the absorbing elements, even at trace levels. XANES spectroscopy has been used for chemical state analyses on a wide range of biological samples [29, 30] and pathological specimens [31, 32].

Synchrotron radiation methods thus enable a new approach in studies about the mechanism of neurodegenerative disorder and cell death by combining the quantitative information of trace metal elements and histological observation at the single cell level. The information obtained in this analysis is significant not only from the viewpoint of therapeutic and medical applications, but also the basic biology concerning the cell death and function of proteins. In this and the following chapter, investigations of parkinsonism-dementia complex, amyotrophic lateral sclerosis and Alzheimer disease are presented as examples of applications of SR in neurodegenerative disorders. The pathology of these diseases is extremely complex and the decisive mechanism responsible for the neuronal cell death remains to be elucidated completely. However, SR based studies are expected to provide innovative data and knowledge about these disorders through high sensitivity elemental and chemical state analysis.

10.2. Parkinsonism-dementia complex

10.2.1. Introduction

Parkinsonism-dementia complex (PDC) and amyotrophic lateral sclerosis (ALS) are prominently found at the three foci in the western Pacific region (Guam, Kii Peninsula and West New Guinea). The neuropathology is characterized by severe neuronal loss and by widespread neurofibrillary tangles (NFT) in affected patients [12]. A major consideration in assessing risk factors has been the relative contribution of genetics and environment to pathogenesis. Comparatively high levels of aluminum and unusually low levels of calcium and magnesium have been found in samples of drinking water and garden soils from Guam and two other high incidence foci of ALS and PDC [23]. The effect of these elemental environments to organism has been investigated by the animal experiments and these experiments demonstrated that the abnormal metabolism of minerals is implicated in the pathogenesis of neurodegenerative disorders [33,34]. It was also revealed in studies on some Guamanian patient [12-13,24,34] that there is prominent accumulation of aluminum and calcium within the nuclear region and surrounding cytoplasm of NFT-bearing hippocampal neurons. The aluminum was reported to yield stable complexes with acids and to produce the accumulation of ammonia that lead to the neuronal death and furthermore it created potential for

Fe-induced oxidative stress [35,36]. But the behavior of transition metal elements in the generation of oxidative stress is poorly understood.

In one study by Shikine et al. (2002), quantitative XRF analysis was performed on substantia nigra (SN) tissues from a patient with Guamanian PDC and a control case. The local distributions and concentrations of intracellular trace metal elements were measured at the single cell level in order to obtain the insight about the neuronal cell death in PDC. The samples from each case were also investigated histologically by staining after XRF analysis.

10.2.2. Sample preparation

In this study by Shikine et al., the samples were brain tissues obtained by autopsy from a 56-year-old male patient with a Guamanian PDC. Autopsies were performed within 88 hours after death and the whole brain without spinal cord was fixed in 10 % formalin. The samples were prepared as thin sections of 8 μm thickness from tissue blocks dissected from pars compacta of the substantia nigra (SN) and embedded in paraffin. The sections were mounted on a mylar film. The SN tissues of an age-matched male patient who died with non-neurological disorder were treated in the same way and were used as a control. Serial sections adjacent to the section used for x-ray analysis were stained by the hematoxylin-eosin staining in order to verify the distribution and extent of NFT involvement.

10.2.3. Experimental procedure and result.

The SR-XRF analyses in this study were performed at Photon Factory in beam line 4A. The incident x-ray energy was 14.3 keV and the beam size was approximately $8 \times 5\ \mu m^2$. The detailed set-up of the beam line is described previously and the analyses were carried out in air. The optical microscope observation of the unstained PDC nigral section indicated that the section contained only a few neuromelanin granules, much fewer than the control. The loss of melanized neurons in the SN is characteristic of PDC [37].

The elemental distribution images were obtained in the areas that contained surviving neuromelanin granules. Figure 10.1 and 10.2 show the elemental images of (b) Fe and (c) Zn and the corresponding (a) microscopic photographs (after staining) obtained from the control and PDC cases respectively. The scale on the right side of the images shows the count of the detector as the fluorescent x-ray intensity. The measurement areas were $190 \times 140\ \mu m^2$, $45 \times 70\ \mu m^2$ and $60 \times 60\ \mu m^2$, and the measurement times were 3 sec/point, 6 sec/point and 7sec/point for figure 10.1, 10.2A

and 10.2B, respectively. The ranges of intensity were from 0 to 41 for Fe and 0 to 44 for Zn in figure 10.1, from 0 to 41 for Fe and 0 to 44 for Zn in figure 10.2A and from 0 to 41 for Fe and 0 to 44 for Zn in figure 10.2B, respectively.

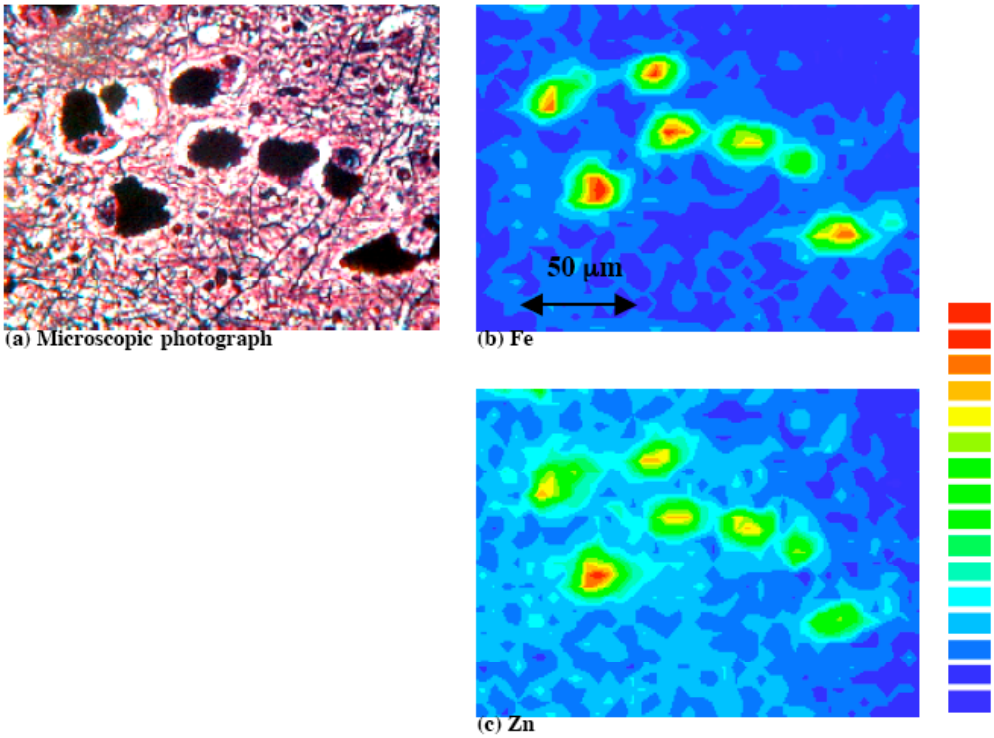

Figure 10.1. The elemental images of (a) Fe and (b) Zn obtained in the substantia nigra tissue from a control case shown in (a) microscopic photograph. Red and blue pixels respectively show areas of high and low intensities. It can be seen that the neurons in the control samples contained Fe and Zn.

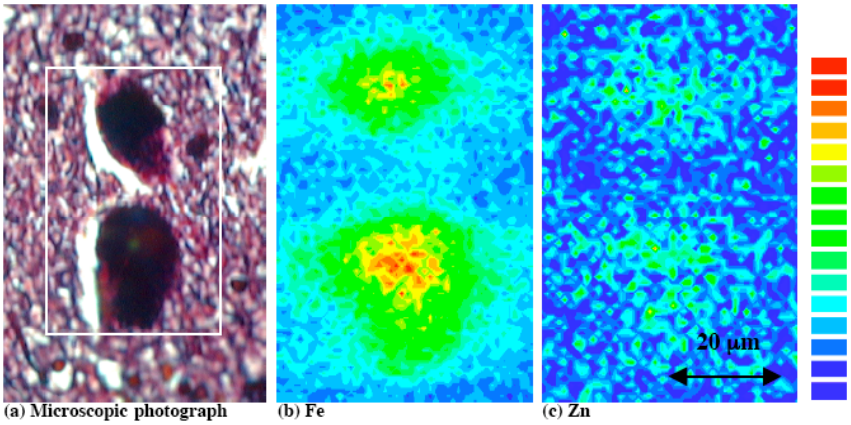

Figure 10.2A. The elemental images of (a) Fe and (b) Zn obtained in the substantia nigra tissue from the PDC case shown in (a) microscopic photograph. White rectangle indicates the region of imaging. It can be seen that the colony contained Fe while the distribution of Zn was hardly detected due to the low concentration.

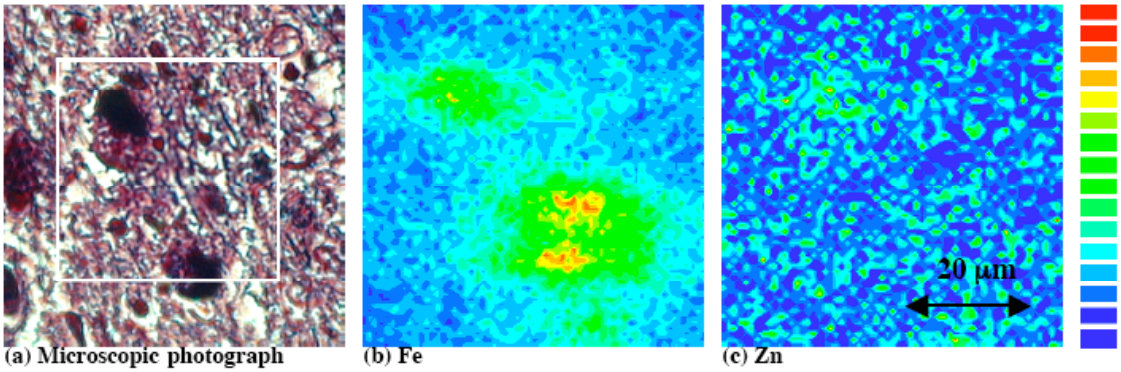

Figure 10.2B. The elemental images of (a) Fe and (b) Zn obtained in the substantia nigra tissue from the PDC case shown in (a) microscopic photograph. It can be seen that the colony contained Fe while the distribution of Zn was hardly detected due to the low concentration.

From the results of the imaging, the measurement points were selected for further point-measurement. The selected points in the control and PDC samples are shown as figure 10.3a and 10.3b, which are the optical microscopic photographs after the staining. In the sample from the control case, the points of A1-3 and B1-2 indicate neuromelanin granules and nigral tissues respectively. XRF spectra were obtained at these points. The typical spectra that were measured in each section are shown in figure 10.4a. The measurement time was 200 seconds. Quantitative analysis was then applied to the spectra and the calculated values for concentrations of Fe, Cu, and Zn are shown in table 10.1a.

The analysis for the sample from the PDC case was performed in the same way as the control case. Measurement points A'1-3, B'1-2 and C'1 in figure 10.3b were determined in neuromelanin granules, nigral tissues and glial cells respectively. The typical XRF spectra obtained in each section from the PDC case are shown in figure 10.4b. The concentrations of Fe, Cu, and Zn that were calculated from spectra and the results are also shown in table 10.1b.

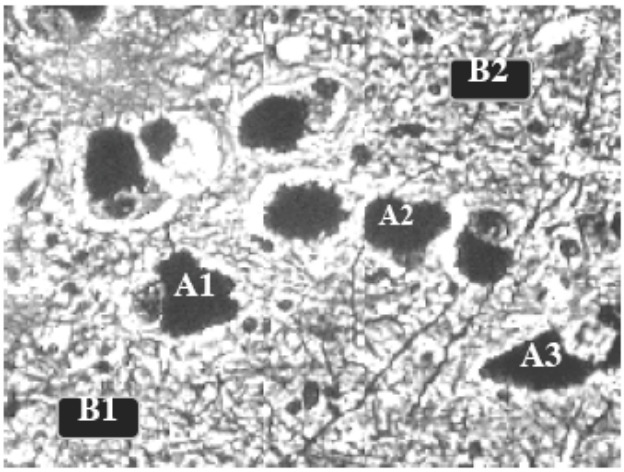

(a) The measurement points in the sample from the control case

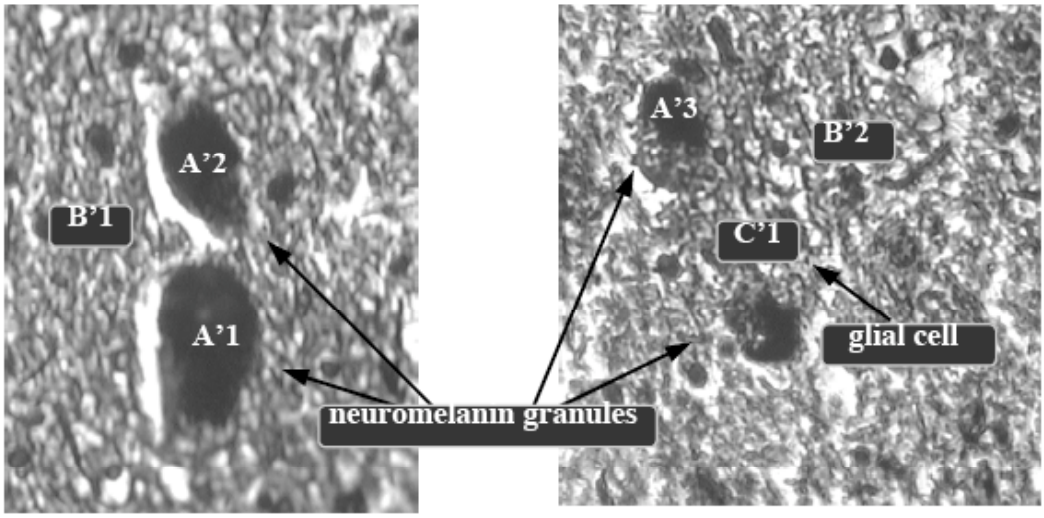

(b) The measurement points in the sample from the PDC case

Figure 10.3. The measurement points selected for quantitative XRF analysis are shown with the optical microscopic photographs of (a) the control sample and (b) the different areas of the sample from the PDC case. The neuromelanin granules, the nigral tissues, and the glial cell are observed at measurement points A (A'), B (B') and C' respectively.

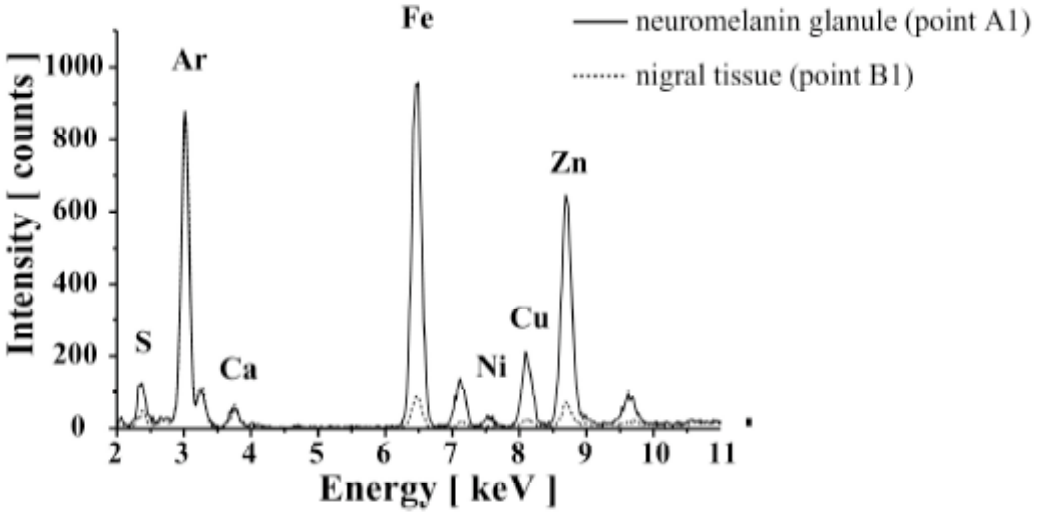

(a) Typical XRF spectra obtained in the sample from the control case

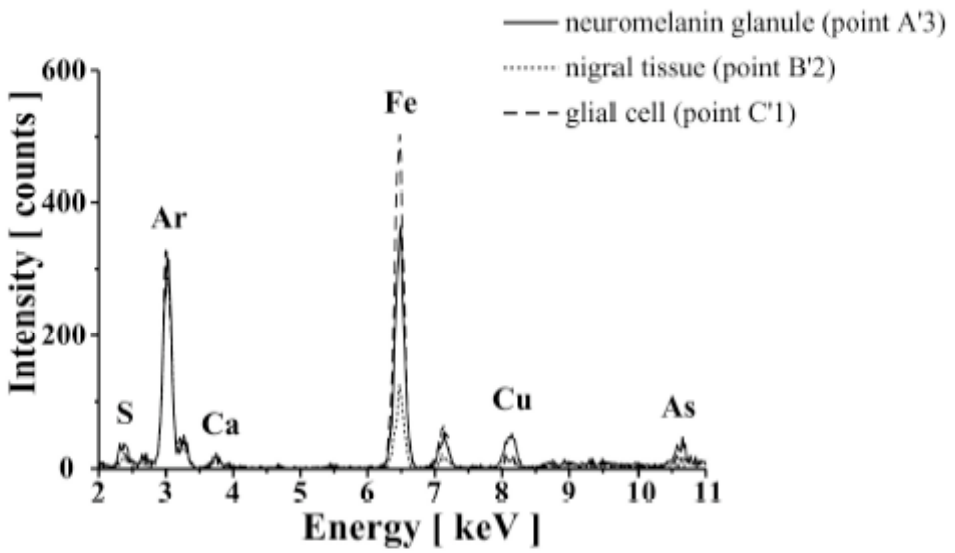

(b) Typical XRF spectra obtained in the sample from the PDC case

Figure 10.4. The typical XRF spectra measured in the substantia nigra (SN) tissues of patients with (a) the control and (b) the Guamanian PDC cases. Measured points in (a) and (b) are shown in figure 10.3. Points A (A'), B (B') and C' are located in the neuromelanin granules, in the nigral tissues, and in the glial cell respectively.

10.2.4. Discussion

Figure 10.1 shows that the neuromelanin granules in the control sample contained more Fe and Zn than the surrounding nigral tissues. The neuromelanin granules in the sample from the PDC case shown in figure 10.2A and 6.2B, however, contained Fe but the Zn contents were not detected because of their low concentrations.

This result was also confirmed by XRF spectrum analysis. The spectra obtained in the neuromelanin granules from the control subject (the typical spectra is shown in figure 10.4a) showed clear peaks of S, Fe, Ni, Cu and Zn, but in the spectra from the PDC case (the typical one is shown in figure 10.4b) Ni and Zn were not detected. On contrary, the peak of As, which was detected in the neuromelanin granules with the PDC case, was not seen in the spectra from the control case. In the spectrum obtained in the glial cell, the high peak of Fe is seen but the peaks of S, Cu, and As are as low as those measured in nigral tissues.

Zn is essential for the function of many enzymes and especially important for neurons because it plays a role of preventing apoptosis induced by free radicals as the active center of Zn/Cu superoxide dismutase (Zn/CuSOD). It is possible that the neurons of the patients affected with PDC are subject to the oxidative stress due to the decrease of Zn/CuSOD. Furthermore, it was revealed in the study about ALS that mutated SOD, which may bind the Zn less robustly, undergo reverse catalysis and produce rather than consume superoxide. The function of generating peroxide and triggering tyrosine nitration of mutant SOD was also reported [5]. These results may be the evidence that these phenomena had actually progressed in the substantia nigra of patients with PDC.

It is widely considered that the neuronal cell death in neurodegenerative disorders is triggered by nutritional deficiencies of Ca and Mg leading to secondary hyperparathyroidism that then facilitates the entry of Ca and toxic heavy metals into the brain [38]. Though Ahlskog et al. analyzed the patients' hair, nail and blood, the evidence of accumulation of heavy elements such as Al, As, Cd, Cu, Fe, Pb, Mg, Hg, and Zn was not found. But in this study, the accumulation of As in neuromelanin granules was clearly shown. Arsenic is a strong vascular toxicant and is possibly the direct cause of neuronal cell death [39]. It is therefore plausible that the abnormal metabolism was induced and the accumulation of As finally occurred and result in the neuronal dysfunction.

XRF elemental imaging shown in figure 10.2Bb indicates that iron accumulated outside of the neuromelanin granules. Hematoxylin-eosin and Bodian stainings after

x-ray analysis revealed that the glial cell was located in this region. The iron had presumably been released from the neuromelanin granule and phagocytosed by the glial cell. McGeer et al. reported that microglia or macrophages had phagocytosed dopaminergic neurons in the SN of postmortem Parkinson's and Alzheimer's disease brains [40,41]. It was revealed that the similar phagocytosis by glial cells had occurred in the tissues of the PDC afflicted patient.

Table 10.1. The quantification results obtained from XRF spectra that were measured of patients with (a) the control and (b) the Guamanian PDC cases.

Measurement points	Concentration [ppm]		
	Fe	Cu	Zn
Neuromelanin granule			
A1	$2.2x10^3$	$2.9x10^2$	$8.1x10^2$
A2	$2.0x10^3$	$1.7x10^2$	$6.3x10^2$
A3	$2.4x10^3$	$1.7x10^2$	$5.6x10^2$
Nigral tissue			
B1	$3.1x10^2$	$9.3x10^1$	$1.4x10^2$
B2	$2.0x10^2$	$3.6x10^1$	$8.0x10^1$

(a) The quantification results from the control case.

Measurement points	Concentration [ppm]		
	Fe	Cu	Zn
Neuromelanin granule			
A'1	$3.1x10^3$	$3.2x10^2$	$<4.0x10^1$
A'2	$2.7x10^3$	$3.0x10^2$	$<4.0x10^1$
A'3	$2.3x10^3$	$2.1x10^2$	$<4.0x10^1$
Nigral tissue			
B'1	$7.3x10^2$	$6.0x10^1$	$<3.0x10^1$
B'2	$7.2x10^2$	$5.2x10^1$	$<2.0x10^1$
Glial cell			
C'1	$3.2x10^3$	$6z.2x10^1$	$<2.0x10^1$

(b) The quantification results from the PDC case.

The results of quantitative XRF analysis shown in table 10.1 indicated that neuromelanin granules of Parkinsonian substantia nigra (SN) contained higher levels of Fe than those of the control. The concentrations were in the ranges of 2300-3100 ppm

and 2000-2400 ppm respectively. On the contrary, Zn and Ni in neuromelanin granules of SN tissue from the PDC case were lower than those of the control. Especially Zn was less than 40 ppm in SN tissue from the PDC case while it was 560-810 ppm in the control. The increase of Fe is considered to be closely related to the neurodegeneration and cell death by promoting the generation of free radicals that induce the oxidative stress.

10.2.5. Conclusion

In summary, from the results of XRF spectroscopy Shikine et al. showed that Fe had accumulated in neuromelanin granules, likely due to the progress of PDC. On the contrary, a reduction of Ni and Zn in the neuromelanin granules was found in the PDC case as compared to the control. In neuromelanin granules the concentrations of Fe were in the ranges of 2300-3100 ppm and 2000-2400 ppm in the PDC and the control cases respectively and for Cu 210-320 ppm and 170-290 ppm respectively. Zn was hardly detected in the PDC case, but in the control case the concentration was 560-810 ppm. In the PDC case, the glial cell adjacent to neuromelanin granules contained Fe with a high concentration of 3200 ppm. Shikine et al. concluded that the decrease of Zn and accumulation of Fe revealed in the sample from the PDC case may be the direct evidence of the generation of the cytotoxicity such as the oxidative stress and tyrosine nitration. The accumulation of As, which is a strong vascular toxicant, was also confirmed in the study. Phagocytosis of the glial cell that was reported in Parkinson's and Alzheimer's brains was observed.

References

1. B. Halliwell, *J. Neurochem.,* **1992**, 59, 1609.
2. S. Fahn, G. Cohen, *Ann. Neurol.,* **1992**, 32, 804.
3. G. Multhaup, A. Schlicksupp, L. Hesse, D. Beher, T. Ruppert, C.L. Masters, K. Beyreuther, *Science*, **1996**, 271, 1406.
4. C.W. Olanow, G.W. Arendash, *Curr. Opin. Neurol.,* **1994**, 7, 548.
5. D.W. Cleveland, J. Liu, *Nature Med*., **2000**, 6, 1320.
6. E.C. Hirsh, J.P. Brandet, P. Galle, Y. Agid, *J. Neurochem*., **1991**, 56, 446.
7. E. Sofic, W. Paulus, K. Jellinger, P. Riederer P, M.B. Youdim, *J. Neurochem*., **1991**, 56, 978.
8. K. Jellinger, E. Kienzl, G. Rumpelmair, P. Riederer, H. Stachelberger, D. Benshachar, M.B. Youdim, *J. Neurochem*., **1992**, 59, 1168.
9. P.F. Good, C.W. Olanow, D.P. Perl, *Brain Res*., **1992**, 593, 343.
10. J.R. Connor, B.S. Snyder, J.L. Beard, R.E. Fine, E.J. Mufson, *J. Neurosci. Res*., **1992**, 31, 327.
11. P.F. Good, D.P. Perl, L.M. Bierer, J. Schmeidler, *Ann. Neurol*., **1992**, 31, 286.
12. D.P. Perl, D.C. Gajdusek, M.G. Garruto, R.T. Yanagihara, C.J. Gibbs Jr., *Science*, **1982**, 217, 1053.
13. R.M. Garruto, R. Fukatsu, R. Yanagihara, D.C. Gajdusek, G. Hook, C.E. Fiori, *Proc. Natl. Acad. Sci. USA*, **1984**, 81, 1875.
14. M. Gerlach, D. Ben-Shachar, P. Riederer, M.B. Youdim, *J. Neurochem*., **1994,** 63, 793.
15. J.R. Connor, "*Evidence for iron mismanagement in the brain in neurological disorders, in Metals And Oxidative Damage In Neurological Disorders*", **1997**, Plenum Press, 23.
16. S.J. Stohs, D. Bagchi, *Free Radic. Biol. Med.,* **1995**, 18, 321.
17. A.I. Bush, *Curr. Opin. Chem. Biol.,* **2000**, 4, 184.
18. P.S.P. Thong, F. Watt, D. Ponraj, S.K. Leong, Y. He, T.K.Y. Lee, *Nucl. Instr. Meth. Phys. Res. B,* **1999**, 158, 349.
19. J.T. Coyle, P. Puttfarcken, *Science*, **1993**, 262, 689.
20. E. Kienzl, L. Puchinger, K. Jellinger, W. Linert, H. Stachelberger, R.F. Jameson, *J. Neurol. Sci.*, **1995**, 134, S69.
21. F. Watt, *Cell. Mol. Biol*., **1996**, 42, 17.
22. C.J. Sparks Jr., "*Synchrotron Radiation Research*", **1980**, ed. H. Winick and S. Doniach, Plenum Press.
23. R.M. Garruto, Y. Yase, *Trends Neurosci*., **1986**, 9, 368.

24. P. Piccardo, R. Yanagihara, R.M. Garruto, C.J. Gibbs, D.C. Gajdusek, *Acta Neuropathol.,* **1988**, 77, 1.
25. G.R. Lachance, F. Claisse, "*Quantitative x-ray fluorescence analysis",* **1995**, ed. J. Wiley & Sons.
26. S. Yoshida, A.M. Ektessabi, S. Fujisawa, *J. Synchr. Rad.,* **2001**, 8, 998.
27. A.M. Ektessabi, S. Fujisawa, K. Takada, K. Yoshida, H. Maruyama, R.W. Shin, *Int. J. PIXE,* **1999**, 9, 297.
28. A.M. Ektessabi, S. Yoshida, K. Takada, *X-ray Spectrom.,* **1999**, 28, 456.
29. A. Bianconi, A. Congiu-Castellano, P.J. Durham, S.S. Hasnain, S. Phillips, *Nature*, **1985**, 318, 685.
30. S. Della Longa, S. Pin, R. Cortès, A.V. Soldatov, B. Alpert, *Biophys. J.,* **1998**, 75, 3154.
31. A.J. Kropf, B.A. Bunker, M. Eisner, S.C. Moss, L. Zecca, A. Stroppolo, P.R. Crippa, *Biophys. J*., **1998**, 75, 3135.
32. P.D. Griffiths, B.R. Dobson, G.R. Jones, D.T. Clarke, *Brain*, **1999**, 122, 667.
33. T. Kihira, S. Yoshida, J. Komoto, I. Wakayama, Y. Yase, *Neurotoxicol.,* **1995**, 16, 413.
34. M. Yasui, Y. Yase, K. Ota, *J. Neurol. Sci.,* **1991**, 105, 206.
35. C.X. Xie, M.P. Mattson, M.A. Lovell, R.A. Yokel, *Brain Res.,* 1996, 743, 271.
36. R. Deloncle, O. Guillard, *Neurochem. Res*., **1990**, 15, 1239.
37. S. Goto, A. Hirano, S. Matsumoto, *Ann. Neurol*., **1990**, 27, 520.
38. J.E. Ahlskog, S.C. Waring, L.T. Kurland, R.C. Petersen, T.P. Moyer, W.S. Harmsen, D.M. Maraganore, P.C. Obrien, C. Estebansantillan, V. Bush, *Neurology*, **1995**, 45, 1340.
39. W. Zheng, *Microsc. Res. Tech.,* **2001**, 52, 89.
40. P.L. McGeer, S. Itagaki, B.E. Boyes, E.G. McGeer, *Neurology,* **1988**, 38, 1285.
41. P.L. McGeer, S. Itagaki, H. Akiyama, E.G. McGeer, *Ann. Neurol.,* **1988**, 24, 574.